Thermo-magneto-convective instabilities in a vertical layer of ferro-magnetic fluid

Sergey A. Suslov, Alexandra A. Bozhko and Gennady F. Putin
ssuslov@usq.edu.au

Abstract

We study convection in a vertical layer of ferro-magnetic fluid heated from the side and subject to a transverse magnetic field. It is found that the subsequent fluid motion is caused by interacting thermo-gravitational and thermo-magnetic mechanisms. Our experiments and computations show that the excitation of magneto-convection leads to the formation of vertically aligned stationary rolls, while gravitational convection results in horizontal rolls corresponding to a pair of counter-propagating thermal waves. The interaction of these instability modes leads to a wide spectrum of experimentally observed flow patterns including stationary rolls and standing waves of various spatial orientations. A comprehensive stability map is computed and compared with experimental flow visualisations. Disturbance energy is analysed to achieve a deeper insight into the physical mechanisms driving the fluid motion.

1   Introduction

Common non-conducting artificial magnetic fluids consist of magnetite colloids which contain ferro-magnetic nano-particles suspended in a carrier fluid, usually synthetic oil, water or kerosene. To prevent formation of magnetite aggregates and their subsequent sedimentation a surfactant such as oleic acid is frequently used [1]. One of the applications of non-conducting ferrofluids is as a heat carrier in efficient cooling systems where the heat transfer by natural gravitational convection can be significantly enhanced by applying an external magnetic field [2]. Nonuniform heating results in a nonuniform magnetisation of a ferrofluid: cooler regions contain stronger magnetised fluid. Subsequently, a ponderomotive force arises which drives stronger magnetised cooler fluid particles to the regions with a stronger magnetic field. This phenomenon is known as magneto-convection and is not associated with gravitational buoyancy forces. However in normal gravity conditions it always acts alongside with the buoyancy forces. Therefore the purpose of the current work is

to use a perturbation energy analysis to determine the parametric regions where each of these physical mechanisms is dominant as well as to determine the internal structure of the corresponding instability patterns. To achieve these goals we choose the simple geometry of a vertical wide and tall fluid layer heated from one side and placed in a perpendicular magnetic field. Such a configuration is easy to re-create experimentally and is convenient to model due to the simplicity of the boundary conditions.

2   Problem definition and stability equations

Consider a vertical layer of ferro-magnetic fluid which fills the gap between two infinitely long and wide parallel plates. The plates are separated by distance $2d$ and are maintained at constant different temperatures $T_* \pm \Theta$. An external horizontal uniform magnetic field $\vec{H}^e = (H^e, 0, 0)$ is applied perpendicular to the layer. This field causes an internal magnetic field $\vec{H}$ within the layer. Since the fluid is ferromagnetic the external field leads to its magnetisation $\vec{M}$ which is assumed to be co-directed with the internal magnetic field: $\vec{M} = \chi_* \vec{H}$, where χ_* is the magnetic susceptibility of the ferromagnetic fluid. We adopt Boussinesq approximation for the governing continuity, Navier-Stokes and thermal energy equations which are complemented by Maxwell's equations for magnetic field as discussed in [1, 2, 3]. The equations are non-dimensionalised using

$$(x', y', z') = d(x, y, z)\,, \quad \vec{v}' = \frac{\eta_*}{\rho_* d}\vec{v}\,, \quad t' = \frac{\rho_* d^2}{\eta_*}t\,, \quad P' = \frac{\eta_*^2}{\rho_* d^2}P\,, \quad T' - T_* = \Theta\theta\,,$$

$$\vec{H}' = \frac{K\Theta}{1+\chi}\vec{H}\,, \ H' = \frac{K\Theta}{1+\chi}H\,, \ \vec{M}' = \frac{K\Theta}{1+\chi}\vec{M}\,, \ M' = \frac{K\Theta}{1+\chi}M\,, \ \vec{g} = g\vec{e}_g\,,$$

where primes denote dimensional quantities. Then we obtain

$$\frac{\partial \vec{v}}{\partial t} + \vec{v} \cdot \nabla \vec{v} = -\nabla P + \nabla^2 \vec{v} - Gr\theta \vec{e}_g - Gr_m \theta \nabla H\,, \tag{1}$$

$$\frac{\partial \theta}{\partial t} + \vec{v} \cdot \nabla \theta = \frac{1}{Pr}\nabla^2 \theta\,, \quad \nabla \cdot \vec{v} = 0\,, \quad \nabla \times \vec{H} = \vec{0}\,, \tag{2}$$

$$(1 + \chi_*)\nabla \cdot \vec{H} + (\chi - \chi_*)\nabla H \cdot \vec{e}_* - (1 + \chi)\nabla \theta \cdot \vec{e}_* = 0\,, \tag{3}$$

$$\vec{M} = [(\chi - \chi_*)(H - N) - (1 + \chi)\theta]\vec{e}_* + \chi_*\vec{H} \tag{4}$$

with boundary conditions

$$\left[\vec{H}^e - [(\chi - \chi_*)(H - N) \mp (1 + \chi)]\vec{e}_* - (1 + \chi_*)\vec{H}\right] \cdot \vec{n} = 0\,, \tag{5}$$

$$\vec{v} = \vec{0}\,, \quad \theta = \pm 1\,, \quad \text{at } x = \mp 1\,, \tag{6}$$

where $\vec{e}_g = (0, -1, 0)$, $\vec{n} = \vec{e}_* = (1, 0, 0)$. The dimensionless parameters appearing in the problem,

$$Gr = \frac{\rho_*^2 \beta_* \Theta g d^3}{\eta_*^2}\,, \ Gr_m = \frac{\rho_* \mu_0 K^2 \Theta^2 d^2}{\eta_*^2(1+\chi)}\,, \ Pr = \frac{\eta_*}{\rho_* \kappa_*}\,, \ N = \frac{H_*(1+\chi)}{K\Theta}\,, \tag{7}$$

are thermal and magnetic Grashof numbers characterising the importance of buoyancy and magnetic forces, Prandtl number characterising the ratio of viscous and

thermal diffusion and parameter N characterising thermo-magnetic properties of a working fluid, respectively. In the above ρ_*, η_* and κ_* are the fluids characteristic density, dynamic viscosity and thermal diffusivity, $\mu_0 = 4\pi \times 10^{-7}$ H/m is the magnetic constant, T_*, M_* and H_* are the temperature, the magnetisation and the magnitude of the magnetic field in the mid-plane of the layer, $\chi = \left.\frac{\partial M}{\partial H}\right|_{H_*}$, $K = -\left.\frac{\partial M}{\partial T}\right|_{T_*}$.

Equations (1)–(6) admit steady parallel basic flow solution

$$\theta_0 = -x\,, \quad v_0 = \frac{Gr}{6}(x^3 - x)\,, \quad P_0 = -Gr_m\frac{x^2}{2} + C\,, \tag{8}$$

$$H_0 = N - x\,, \quad M_0 = \chi_* N + x\,, \tag{9}$$

where C is an arbitrary constant. The buoyancy force caused by the linear variation of the temperature (and the density) across the layer are responsible for the existence of a symmetric cubic velocity profile such that the fluid rises along the hot wall and sinks along the cold one. The fluid magnetisation increases towards the cold wall while the magnetic field decreases in this direction so that the sum $H_0 + M_0 =$const. as dictated by Maxwell's equations in the absence of electrical currents.

As shown in [4] linearising equations (1)–(6) about (8)–(9), and then using a standard normal mode decomposition of the disturbance fields and Squire's transformation we obtain an equivalent two-dimensional stability problem of the form

$$\sigma u \;+\; \left(\alpha^2 + i\alpha v_0 - D^2\right)u + DP + Gr_m DH_0\,\theta + Gr_m\Theta_0 D^2\phi = 0\,, \tag{10}$$

$$\sigma v \;+\; Dv_0\,u + \left(\alpha^2 + i\alpha v_0 - D^2\right)v + i\alpha P - Gr\theta + i\alpha Gr_m\Theta_0 D\phi = 0\,, \tag{11}$$

$$\sigma\theta \;+\; D\Theta_0 u + \left(\frac{\alpha^2 - D^2}{Pr} + i\alpha v_0\right)\theta = 0\,, \tag{12}$$

$$Du + i\alpha v = 0\,, \quad \left(D^2 - \frac{1 + \chi_*}{1 + \chi}\alpha^2\right)\phi - D\theta = 0\,, \tag{13}$$

with boundary conditions

$$u_1 = v_1 = w_1 = \theta_1 = 0\,, \quad (1 + \chi)D\phi_1 \pm \sqrt{\alpha^2 + \beta^2}\phi_1 = 0 \quad \text{at } x = \pm 1\,, \tag{14}$$

where $D \equiv d/dx$ and ϕ is the magnetic potential such that the disturbance magnetic field is given by $\vec{H} = (D\phi, i\alpha\phi)$. All disturbance quantities in equations (10)–(13) are functions of x only, see [3, 4] for details. Equations (10)–(14) comprise an eigenvalue problem for the disturbance complex amplification rate $\sigma = \sigma^R + i\sigma^I$ for each fixed set of governing physical parameters and wavenumber α. Marginal stability is observed when the value of σ^R maximised over the range of α becomes zero.

We emphasise that two-dimensional perturbation equations (10)–(14) represent a full three-dimensional problem which is recovered using the inverse Squire's transformation. However the goal of this short paper is to determine the physical mechanisms driving the instabilities which is possible to do by using a two-dimensional equivalent problem alone. The reader is referred to [4] for the detailed analysis of the three-dimensional unfoldings of the current results.
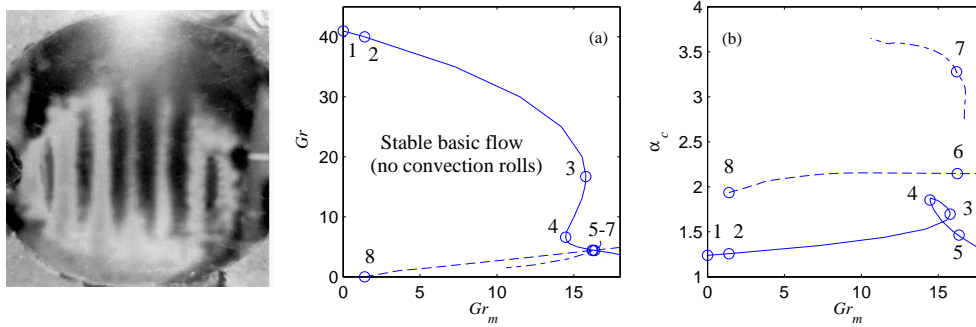
Figure 1: Typical experimentally observed magneto-convective instability pattern (left), parametric stability boundary (a) and critical wavenumber (b) for combined thermo-gravitational and magnetic convection in a vertical layer of ferro-fluid at $Pr = 130$ and $\chi = \chi_* = 5$. Basic flow is stable below and to the left of the solid line and above the dashed and dash-dotted lines in plot (a).

3 Instability mechanisms and disturbance energy

Experimental observations [5] show that various types of instability patterns superposed onto the basic flow exist depending on the values of the governing parameters. The most prominent pattern has the form of vertical rolls such as the ones seen in the left photo in Figure 1. Computations show that it appears for $Gr_m > 1.39$, relatively small values of Gr and wavenumber $\alpha_c \approx 1.9$ (dashed lines in Figure 1(a,b)). These values are in good agreement with the experimentally measured ones at the onset of instability. However computations also predict the existence of other instabilities for the larger values of Gr_m (dash-dotted line in Figure 1(a)) and Gr (solid line).

In order to determine the physical mechanisms driving instabilities we consider the disturbance energy balance. We multiply the momentum equations (10) and (11) by complex conjugate velocity components $\bar{u}$ and $\bar{v}$, respectively, add them together, integrate by parts across the layer using boundary conditions (14) and the continuity equation, and take the real part (denoted by $\Re$ below) of the result to obtain

$$\sigma^R \Sigma_k = \Sigma_{uv} + \Sigma_{m1} + \Sigma_{m2} + \Sigma_{Gr} + \Sigma_{vis} \,, \tag{15}$$

where

$$\Sigma_k = \int_{-1}^{1} \left(|u|^2 + |v|^2 \right) dx > 0 \,, \quad \Sigma_{uv} = - \int_{-1}^{1} Dv_0 \Re(u\bar{v}) \, dx \,,$$

$$\Sigma_{m1} = \int_{-1}^{1} \underbrace{-Gr_m DH_0 \, \Re(\theta\bar{u})}_{E_{m1}} \, dx \,, \quad \Sigma_{m2} = \int_{-1}^{1} \underbrace{Gr_m D\theta_0 \, \Re(D\phi\,\bar{u})}_{E_{m2}} \, dx \,, \tag{16}$$

$$\Sigma_{Gr} = \int_{-1}^{1} \underbrace{Gr\Re(\theta\bar{v})}_{E_{Gr}} \, dx \,, \quad \Sigma_{vis} = - \int_{-1}^{1} \left(|Du|^2 + |Dv|^2 \right) dx < 0 \,.$$

Since Σ_k, the kinetic energy of perturbations, is positively defined the flow is stable (unstable) if the sum of terms in the right-hand side of (15) is negative (positive).

Table 1: Disturbance energy integrals for selected marginal stability points shown by circles in Figure 1.

	Gr_m	Gr	α	Σ_{uv}	Σ_{m1}	Σ_{m2}	Σ_{Gr}
1	0	40.974	1.238	-0.006	0	0	1.006
2	1.398	39.976	1.256	-0.007	0.004	-0.002	1.005
3	15.775	16.690	1.696	-0.011	0.302	-0.086	0.795
4	14.468	6.6	1.853	-0.003	1.141	-0.318	0.180
5	16.353	4.4	1.463	0.001	1.795	-0.759	-0.036
6	16.239	4.4	2.147	0.002	1.812	-0.595	-0.219
7	16.189	4.4	3.278	-0.003	1.516	-0.350	-0.163
8	1.398	0	1.936	0	1.584	-0.584	0

Equivalently, we can say that positive terms in the right-hand side of (15) are responsible for instability. The values of various energy balance terms are given in Table 1 for the marginal stability ($\sigma^R = 0$) points shown by circles in Figure 1(a,b). Since within the framework of a linearised stability analysis the amplitude of disturbance fields is undefined we normalise them in such a way that the viscous dissipation integral $\Sigma_{vis} = -1$ for all points. The remaining four entries in the energy balance are listed in Table 1. From this table we make the following conclusions.

- The contribution of the basic flow velocity into the disturbance energy balance (Σ_{uv}) can be either slightly positive or negative, but it remains small for all regimes. Therefore the interaction of the disturbance velocity field with the basic flow is weak. The energy exchange between basic and disturbance velocity fields is insignificant and does not play any noticeable role in flow pattern formation.

- The first of the two magnetic contributions to the energy balance, Σ_{m1}, is positive for all non-zero values of Gr_m. This term represents a ponderomotive force which drives stronger magnetised cooler fluid particles into the regions of a stronger basic magnetic field (i.e. from the cold wall towards the hot wall as suggested by the basic flow field distributions (8)–(9)). Therefore in the considered configuration the dependence of fluid magnetisation on the temperature always plays a destabilising role leading to the onset of a thermo-magnetic convection.

- In contrast, the second magnetic term, Σ_{m2}, always remains negative. It represents the induction of a disturbance magnetic field by displaced ferro-magnetic fluid particles. Therefore the modification of the basic magnetic field always absorbs energy and thus plays a stabilising role. It hinders the change in the primary magnetisation field. However this magnetic stabilisation effect is always weaker than the thermo-magnetic de-stabilisation. Therefore the overall magnetic influence on the basic flow in the considered geometry is always destabilising.

- The thermo-gravitational contribution, Σ_{Gr}, depends strongly on the values of both Gr and Gr_m and can be either positive or negative. This term represents
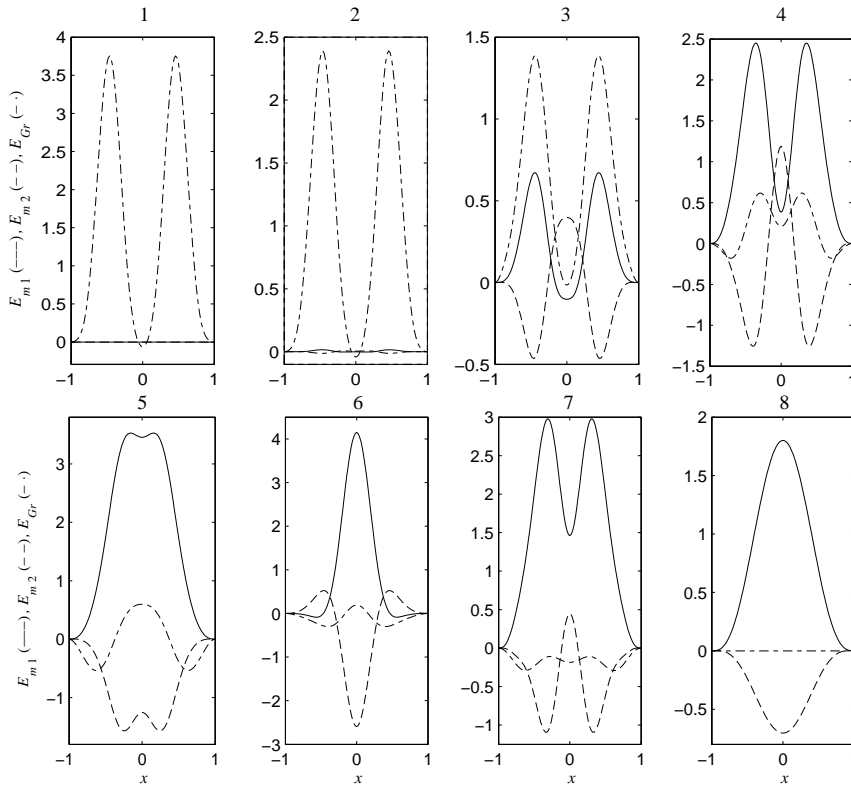
Figure 2: Selected disturbance energy integrands for parameters specified in Table 1.

the buoyancy force which drives warmer and less dense fluid upwards and cooler denser fluid downwards. It is strongly destabilising in the absence of a magnetic field i.e. for $Gr_m \sim 0$, but becomes stabilising for the larger values of Gr_m when the motions caused by the actions of the vertical buoyancy force and the horizontal magnetic ponderomotive force start competing with each other. The peculiar S-shape of the stability boundary shown by the solid line in Figure 1(a) is the consequence of this competition: for larger values of Gr both magnetic and thermo-gravitational terms are destabilising and their combination leads to a reduction in the area of the region of stability (the solid line goes down and then turns back). However for small values of Gr and larger values of Gr_m the buoyancy starts playing a much stronger stabilising role so that the solid line turns to the right increasing the stability region underneath it.

In summary, the de-stabilisation of the primary parallel flow is achieved due to the action two physical mechanisms: the action of ponderomotive magnetic and buoyancy forces. However at small values of Gr the buoyancy plays a stabilising role. The integral values presented in Table 1 also identify the nature of the instabilities whose boundaries are shown by the solid and dashed lines in Figure 1: gravitational buoyancy and magnetic ponderomotive force, respectively. Yet neither the details of these two instabilities nor the nature of the third instability whose boundary is shown by the dash-dotted line are clear so far. In order to eliminate this shortcoming

we consider the spatial distribution of the three destabilising integrands, E_{m1}, E_{m2} and E_{Gr}, defined in (16) and plotted in Figure 2 for points 1–8 shown by circles in Figure 1(a,b).

For small values of Gr_m and large values of Gr (points 1 and 2) the thermo-gravitational instability mechanism dominates, see the dash-dotted line in plots 1 and 2 in Figure 2. The energy integrand E_{Gr} has two well defined symmetric maxima near the walls. This is a reflection of the well known fact that in high Prandtl number fluids such as a typical kerosene-based ferro-colloid the thermo-gravitational instability takes the form of two counter-propagating waves in the wall regions, see detailed discussion in [4] and references therein. They are almost insensitive to a magnetic field and exist even when the magnetic Grashof number is significantly increased, see plots for points 3 and 4. However as the ratio Gr_m/Gr increases the thermo-magnetic effects given by E_{m1} intensify significantly and eventually become dominant, see plot 4. It is noteworthy that although the dominant physical mechanism of instability changes, this happens in a continuous way, see solid lines in Figure 1. The only indication that such a change has indeed occured is in the qualitative behaviour of the disturbance wavenumber: as Gr_m increases so does the wavenumber of thermo-gravitational waves, however this trend is reversed once they are replaced with thermo-magnetic waves, see the solid line in Figure 1(b).

With decreasing Gr the difference between the two counter-propagating thermo-magnetic waves becomes blurred: the wave speeds (not shown here, but see [4]) decrease, the instability pattern becomes nearly stationary and its maximum shifts from the wall regions towards the centre of the layer, see the plot for point 5. The thermo-gravitational convection mechanism continues to play a destabilising role in the centre of the layer, but its influence in the wall regions becomes stabilising. A shift of the instability production region to the centre of the layer has a profound effect on the characteristic wavenumber of perturbations: it quickly decreases, see the right end of the solid line in Figure 1(b). This has a straightforward explanation: the disturbance structures in the centre of the layer near the inflection point of the basic flow velocity profile are subject to large shear forces. They "stretch" convection rolls decreasing their wavenumber. The centrally located instability structures elongated by the shear forces then become so large that they cause a strong "flow blocking" effect. Eventually they are destroyed by the basic flow giving way to much shorter structures, see the dash-dotted lines containing point 7 in Figure 1. Plot 7 in Figure 2 shows that the physical mechanism generating them is indeed the same as that for the thermo-magnetic waves discussed above. Their size is sufficiently small (the wavenumber is large) for the basic flow blocking effect to be reduced on one hand and for the two disturbance waves propagating near the walls to re-appear on the other. We also note that although overall magneto-induction effect Σ_{m2} is always stabilising, the energy integrand E_{m2} for points 3, 4 and 7 is positive in the centre of the layer (between the counter-propagating thermo-magnetic waves) and thus it contributes to the overall de-stabilisation across the layer.

Points 6 and 8 in Figure 1 belong to the third type of stability boundary which is disjoint from the two segments discussed so far. The physical mechanism causing this instability is of purely thermo-magnetic type: E_{m2} is strongly positive while E_{Gr} is close to zero. Therefore the gravitational buoyancy plays essentially no role

in these regimes of convection. Major de-stabilisation occurs near the middle of the layer where basic flow velocity is zero. As a consequence, these corresponding instability patterns are stationary [4]. They take the form of vertical rolls similar to the ones seen in the left photograph in Figure 1.

In conclusion, our analysis of perturbation energy distribution across the layer shows that the instability in a vertical ferro-fluid layer is caused by two physical mechanisms: thermo-gravitational (buoyancy) and thermo-magnetic. These mechanisms result in three distinct types of perturbed flow patterns: counter-propagating thermal waves (large Gr, small Gr_m), counter-propagating thermo-magnetic waves (large Gr_m, intermediate Gr) and stationary magneto-convection rolls (intermediate to large Gr_m, small Gr). The transition between thermal and thermo-magnetic waves is continuous and occurs when Gr and Gr_m are of comparable sizes while magneto-convection rolls appear independently and dominate the flow for small values of Gr. We also note in passing that a spatial orientation of the detected instability patterns is strongly related to the physical mechanisms causing them: the propagating thermal or thermo-magnetic instability waves form horizontal or inclined convection rolls, while stationary magneto-convection rolls are vertical. The reader is referred to [4] for detailed discussion of the spatial structure of instability patterns.

Acknowledgements

References

[1] E. Ya. Blums, M. M. Maiorov and A.O. Tsebers. Magnetic Fluids, Zinatne, Riga, Latvia (in Russian), 1989.

[2] V. G. Bashtovoy, B. M. Berkovsky and A. N. Vislovich. Introduction to thermo-mechanics of magnetic fluids. Published by the Institute of High Temperatures of the Russian Academy of Sciences, Moscow, Russia (in Russian), 1985.

[3] B. A. Finlayson. Convective instability of ferromagnetic fluids. *J. Fluid Mech.*, **40**, 753–767, 1970.

[4] S. A. Suslov. Thermo-magnetic convection in a vertical layer of ferromagnetic fluid. Submitted to *Phys. Fluids*, 2008.

[5] A. A. Bozhko and G. F. Putin. Experimental investigation of thermo-magnetic convection in uniform external field, *Izvestiya Academii Nauk SSSR (Letters of the Academy of Sciences of USSR)* (in Russian), **55**, 1149–1156, 1991.

Sergey A. Suslov, Department of Mathematics and Computing, University of Southern Queensland, Toowoomba, Queensland 4350, Australia.

Alexandra A. Bozhko and Gennady F. Putin, Department of General Physics, Perm State University, 15 Bukirev St., Perm, 614600, Russia.